USING REMOTE SENSING DATA FOR POST-FIRE RECOVERY ANALYSIS

Kowalski, Kyleigh, GIS Technician, ISU GIS Training and Research Center
Weber, Keith, GIS Director, ISU GIS Training and Research Center

Abstract

The spatiotemporal recovery of vegetation within burned areas is a complex process that land managers go to great lengths to monitor and understand. When coupled with *in situ* field observations, remote sensing imagery, such as NDVI and dNBR, along with LiDAR data, can help land managers better understand the long-lasting effects of fire on an ecosystem. This study assesses how remotely sensed data can be used to quantify post-fire recovery of burned areas and applies these methods to 17 study fires across the Western US. We primarily focused on trends in post-fire NDVI as a method for assessing ecological recovery across grasslands, shrublands, and forests. Our findings suggest NDVI alone is not a suitable indicator of post-fire recovery due to limitations in capturing structural changes that occur to burned vegetation. However, when NDVI is used in conjunction with fire severity data (e.g., dNBR), LiDAR-derived vegetation height models, and field validation surveys, then land manager can achieve a much more comprehensive view of post-fire recovery. We found pre- and post-fire LiDAR data were essential for determining the structural recovery of vegetation across a landscape. When considered alongside field observations, these remote sensing techniques offer a better understanding of post-fire recovery. The ability to quantify post-fire recovery using remote sensing techniques can help land managers develop well-informed and effective post-wildfire recovery plans.

Keywords: NDVI, LANDSAT, LiDAR, wildfire, fire severity, vegetation

Introduction

This study utilized Normalized Difference Vegetation Index (NDVI), differenced Normalized Burn Ration (dNBR) and Light Detection and Ranging (LiDAR) data to better understand temporal trends in vegetation recovery against fire severity. Remotely sensed data can be leveraged to guide post-fire response teams, such as USDA Forest Service Burned Area Emergency Response (BAER) assessment teams, tasked with mitigating landscape degradation through burned-area rehabilitation and long-term restoration efforts (National Interagency Fire Center (NIFC), n.d.). Monitoring past and current spatiotemporal trends in vegetation productivity relative to wildfire events is beneficial for optimizing recovery plans, quantifying recovery goals, and avoiding unnecessary resource expenditure on attempts to restore landscapes to unattainable or unsustainable conditions. Spatiotemporal patterns of NDVI can provide insights into the persistence and resilience of vegetation in response to known disturbances such as wildfires (Lacouture et al., 2020). NDVI estimates vegetative health; healthy, photosynthetically active vegetation shows stronger near-infrared (NIR) reflectance, while unhealthy vegetation exhibits greater reflectance in the visible red band (R) compared to NIR. Thus, NDVI values nearing 1.0 signify healthy, dense vegetation, while NDVI values nearing 0 represent unhealthy, sparse, dormant, and/or dead vegetation biomass. NDVI values approaching -1.0 tend to indicate water bodies, urbanized areas, or otherwise barren land (NASA Earth Observatory, 2000).

It is difficult to define or quantify what post-wildfire recovery means because recovery looks different across ecosystems and depends on ecosystem resilience, fire severity, and post-fire weather conditions. Recently, a correlation ($R^2 = 0.49$) between canopy cover loss and burn severity has been reported (Epstein et al., 2024). This relationship was used to characterize recovery as the rate at which canopy cover returned to pre-fire conditions. Similarly, NDVI response may be a useful measurement to quantify the effects of fire on a landscape, especially when paired with a fire severity model such as the differenced normalized burn ratio (dNBR), and other land cover data collected *in situ* from within the burned area.

This study characterized NDVI trends for 17 wildfires within three general land cover types (grass-dominant, shrub-dominant, and forest-dominant) in order to assess post-fire recovery across land cover types. However, since NDVI does not provide information on vegetation type, solely using this index may falsely indicate recovery in instances where trees or shrubs have been replaced by rapidly growing grasses that may produce similar NDVI values. To reduce such false positive errors, LiDAR data was utilized to visualize and characterize vegetation structure and changes in canopy height across burned areas where both pre- and post-fire LiDAR data was available.

The rate or time required to affect ecosystem recovery after a disturbance is dependent upon the extent and severity of the disturbance. Thus, fire severity–using dNBR–was considered. Low-severity fires in forested ecosystems are likely to experience less vegetation loss and less land-cover change as existing, mature trees may survive the fire, especially those that are fire-adapted, such as the Ponderosa Pine *(Pinus ponderosa)*. In contrast, high-severity fires may remove entire forests, making the landscape more vulnerable to a land-cover change transition. After major disturbances such as fire, secondary succession occurs, a natural process by which species return to the landscape in stages based on factors related to germination, growth rate, and adaptation to fire (Western Fire Chiefs Association, 2023). During the first stage of succession, the landscape is dominated by species known as post-fire specialists, which may be ferns and mosses. Within a short period of time, many herbaceous plant species will return and thrive without shading from a forest canopy. Over the next several years, tree seedlings begin to sprout and a full forest canopy may be re-established in just a few decades (USDA Forest Service, n.d.). However, the transition from pre-fire forests to post-fire shrublands and grasslands, especially in dry, low elevations, is particularly concerning. Shrub and grassland ecosystems tend to have lower fire return intervals which may lead to more frequent fires that may further reduce forest cover or effectively change the ecosystem type in a region (Stevens-Rumann & Morgan, 2019). In a previous study of post-fire tree regeneration across the Western US, researchers identified over 150 burned forest areas where very few seedlings, if any, were recruited within the burned area (Stevens-Rumann & Morgan, 2019). Their research suggested these forested areas are being replaced primarily by shrubs and grasses as a result of changing climate coupled with intense ecological disturbance from the wildfire. Overall, burned areas with low tree recruitment were most common in dry, low-elevation forests, but were also found in several wet, high-elevation forests (Stevens-Rumann & Morgan, 2019). In order to meaningfully interpret post-fire recovery, an understanding of fire severity and land cover type is essential in conceptualizing how NDVI and LiDAR are able to characterize change across a burned landscape.

Methods & Materials

Study area

This study examined 17 wildfires across the western United States (**Figure 1**). Information describing the fire year, name, state, acres burned, GACC region, peak growing season, and cause were recorded (Table 1). For each fire, the final fire perimeter was acquired from the Historic Fires Database (HFD) (Weber, 2024) and used to calculate spatial statistics for NDVI, land cover, and fire severity (i.e., dNBR).

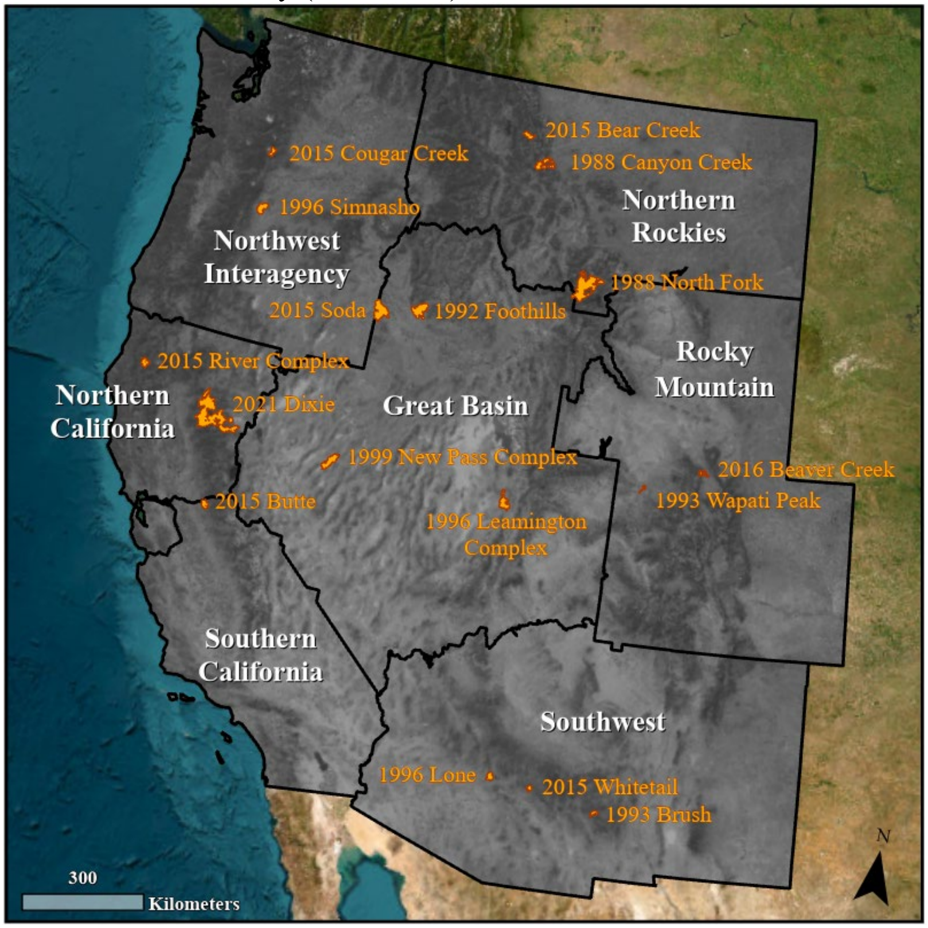

Figure 1. The 17 wildfires examined in this study and seven GACC regions as delineated by the National Interagency Fire Center (2024). Each of the 17 study fires are shown and labeled with the year and fire name.

Data Acquisition & Processing

For study fires occurring after 2012 (*n* = 8), the NDVI Baseline dataset developed by NASA RECOVER was used. Alternatively, fires that burned prior to 2012 (*n* = 9), Landsat 4-5 TM (1982-2011) and Landsat 8-9 TM (2013-2025) Collection 2 Level 2 products were acquired using the USGS Earth Explorer. Next, these images were converted to NDVI using the formula (NIR-SWIR)/(NIR+SWIR). For each study fire, NDVI was acquired for a single date each year from within the peak growing season. In some cases, imagery could not be acquired during the peak growing season due to cloud cover. In these cases, the next nearest clear image to the growing season was used. When there were multiple clear images within the peak growing season for a given year, the image with the highest apparent greenness was selected based on visual observation of the image. The peak growing season months were determined by NDVI trends across Geographic Area Coordination Centers (GACC) regions for each fire (**Table 1**; **Figure 2**; Kowalski & Weber, 2024). NDVI data collection began up to two years prior to the fire start date and continued through 2024. This was done to allow comparison of changes in growing season NDVI for the years immediately prior to and following the fire.

Table 1. Description of each fire explored in this study, including the fire year, name, state, acres burned, GACC region, peak growing season months within the GACC, and cause of the fire. Fires are sorted by fire year (oldest to most recent.

FIRE YEAR	FIRE NAME	STATE	ACRES	GACC	PEAK GROWING SEASON	FIRE CAUSE
1988	North Fork	WY	565,116	Northern Rockies	June/July	Human-caused
1988	Canyon Creek	MT	167,875	Northern Rockies	June/July	Lightning
1992	Foothills	ID	228,076	Great Basin	June/July	Lightning
1993	Brush	NM	39,349	Southwest	August/September	Lightning
1993	Wapati Peak	CO	20,857	Rocky Mountain	June/July	Unknown
1996	Leamington Complex	UT	158,029	Great Basin	June/July	Lightning
1996	Simnasho	OR	117,964	Northwest	July/August	Human-caused
1996	Lone	AZ	60,574	Southwest	August/September	Human-caused
1999	New Pass Complex	NV	172,226	Great Basin	June/July	Lightning
2015	Soda	ID	283,626	Great Basin	June/July	Lightning
2015	River Complex	CA	77,414	Northern California	June/July	Lightning
2015	Butte	CA	70,854	Southern California	June/July	Powerline
2015	Bear Creek	MT	67,292	Northern Rockies	June/July	Lightning
2015	Cougar Creek	WA	53,584	Northwest	July/August	Lightning
2015	Whitetail	AZ	33,626	Southwest	August/September	Lightning
2016	Beaver Creek	CO	38,395	Rocky Mountain	June/July	Human-caused
2021	Dixie	CA	963,405	Northern California	June/July	Powerline

Pre-fire NDVI conditions were estimated by extracting the median statistic from the NDVI Baseline dataset within each fire perimeter (NASA RECOVER, 2023; Schnase et al., n.d.). This method of estimating pre-fire conditions may not be perfectly representative of areas that have burned repeatedly within the last decade, however median NDVI is a resilient statistic and less likely to show this effect compared to the mean. We graphed both median and maximum NDVI Baseline statistics against the growing season NDVI values for each year following the fire.

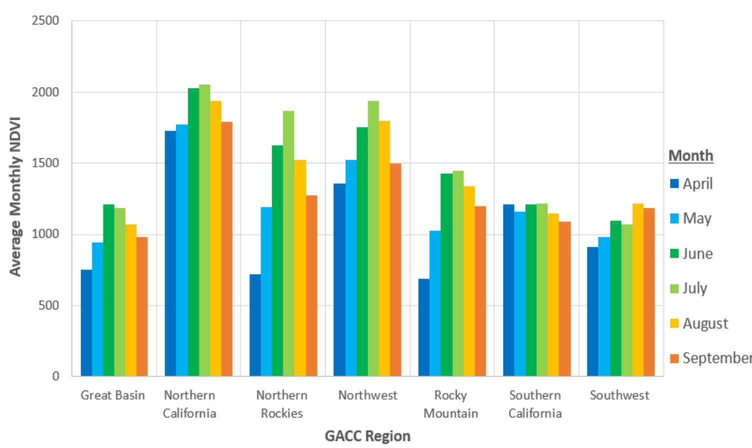

Figure 2. Average monthly NDVI values within each of the 7 GACCs using data from 2013-2022. Blues represent late spring, greens represent early summer, and orange represents late summer. NDVI values and their corresponding dates were extracted from the multidimensional NDVI Baseline and averaged for each month. NOTE: NDVI values have been scaled by a factor of 10,000.

Dominant land cover was characterized within each fire perimeter using the Existing Vegetation Type (EVT) dataset provided by LANDFIRE (2023). Within each fire perimeter, the percent of land cover type was acquired for two fields, vegetation subclass (SBCLS) and Society of American Foresters/Society for Range Management cover type (SAF SRM). Using these data, two land cover pie charts were created for each study fire which help to visualize the relative percent of the top five landcover classes in each respective category. These charts provided a better understanding of landscape conditions at the time the EVT model was developed, but should be interpreted with some caution as there are many assumptions and generalizations associated with such spatially extensive models. These pie charts were used to describe each study fire as grass-dominant, shrub-dominant, or forest-dominant based on the general dominant vegetation and cover types.

In order to investigate the influence of fire severity, dNBRs were calculated for each study fire. The dNBR is the difference between the pre-NBR and post-NBR. The timing of pre- and post-fire imagery collection is important due to the natural phenological differences occurring between years and between landscapes. To best assess change relative to fire, all factors effecting change should be eliminated save for the fire itself. To achieve this, pre- and post-fire imagery were collected within similar phenological stages to minimize seasonal changes in vegetation. Given limitations imposed by satellite return intervals, the atmospheric effects of the fire, and the timing and duration of the fire itself, it was difficult to acquire suitable imagery that eliminated natural phenological change. Rather than trying to acquire pre- and post-fire imagery immediately bounding a fire occurrence, longer-term comparisons were found to be suitable and possibly more effective at determining change and recovery. Using this approach, suitable pre-fire images were acquired from within the growing season of the fire year. The post-fire image was acquired within the growing season of the following year using a phenological synchronization approach (USDA Forest Service, 2006; Weber, 2001).

NBRs were calculated using the near-infrared (NIR) and short-wave infrared (SWIR) bands of an image as follows: (NIR-SWIR)/(NIR+SWIR). The NIR and SWIR bands are used in the Normalized Burn Ratio calculation because these spectral bands change more in response to fire effects than other spectral bands and respond in opposite ways (USDA Forest Service, 2006). Across forested ecosystems, NIR generally exhibits a strong decrease in post-fire imagery while SWIR exhibits a strong increase. The effects of fire do not always lead to the loss of vegetation which would typically lead to a decrease in reflectance. In some cases, fire enhances ecological productivity and reflectance is actually increased in the post-fire imagery. This most commonly occurs in herbaceous and grassy areas where the vegetation can grow back quickly in response to fire-associated nutrient availability. However, the opposite is expected for forested and shrubland regions where re-growth of the established vegetation is likely to be much slower. This contrast between the bands and their ability to capture both positive and negative changes in reflectance post-fire is what makes the NBR effective at identifying burned areas across a variety of landscapes (USDA Forest Service, 2006).

Pre- and post-fire images were acquired as close to the start date and containment date as possible for each fire while avoiding interference from smoke or clouds. Images were acquired using USGS Earth Explorer for Landsat 8-9 Collection-2 Level-2 Surface Reflectance imagery (fires burned after 2012) or Landsat 4-5 Collection-2 Level-2 Surface Reflectance imagery (fires burned prior to 2012). When necessary, scenes were mosaiced before calculating dNBR. In the case of the Soda fire, suitable post-fire imagery could not be found through the Landsat collections. Instead, four scenes of Sentinel-2 L2A Surface Reflectance imagery were acquired and mosaiced together in order to calculate the post-fire NBR. For this reason, the Sodar Fire dNBR is a mixed sensor dNBR and is not directly comparable to the Landsat-derived dNBRs, despite using the same workflow. The use of mixed sensors to create a single satellite-image product introduces uncertainty, as the two sensors have not been harmonized or properly aligned (Ju et al., 2025). For each fire, dNBRs were classified into seven fire severity thresholds: high, moderate-high, moderate-low, low, unburned, enhanced regrowth-low, and enhanced regrowth-high. These fire severity thresholds were defined by the USGS (**Table 2**).

Table 2. Fire severity classes for dNBRs as proposed by the USGS.

Severity Level	**dNBR Range** (scaled by 10^3)
Enhanced Regrowth, high (post-fire)	-500 to -251
Enhanced Regrowth, low (post-fire)	-250 to -101
Unburned	-100 to 99
Low Severity	100 to 269
Moderate-low Severity	270 to 439
Moderate-high Severity	440 to 659
High Severity	660 to 1300

Case Study: 2021 Dixie Fire

The 2021 Dixie fire in California was selected as a focused case study fire for this research. Pre- and post-fire LiDAR was available for the Dixie fire, providing a unique opportunity to assess changes in canopy height relative to NDVI trends, fire severity, and land cover type. We acquired 2018 pre-fire LiDAR (USGS, 2018) and 2022 post-fire LiDAR (USGS, 2022).

Upon visual inspection of the LiDAR point cloud, clusters of data points both high above and far below actual ground surface were detected. The high clusters were likely from birds and we speculate the low clusters may be data anomalies or errors. These clusters were filtered out using a denoising process with LAS Tools where all data points 50 m above and 3 m below the surface were removed from both datasets. After denoising, the original LAS files were converted to raster tiles, mosaicked together, and clipped to the fire perimeter to create Digital Surface Models (DSMs) of pre- and post-fire conditions. The authors note that there were areas within the fire perimeter with incomplete LiDAR coverage for 2022. Data in these areas were set to a height above surface equal to zero. Then, the 2018 DSM was subtracted from the 2022 DSM to create a change detection model for canopy height, where loss in height post-fire is represented as negative values and post-fire gain is represented by positive values. Statistics were calculated on the resulting change detection model by running zonal statistics within each of the fire severity classes to determine the statistical difference between canopy height change across each of the severity classes.

NDVI and dNBR data were processed twice for the 2021 Dixie Fire. Once using imagery from the Landsat 8 & 9 Collection-2 Level-2 as described above and as is consistent with the other 16 study fires, and again using satellite imagery from Landsat 8 & 9 Collection-2 Level-1. During this study, it became apparent that there may be an issue in the Landsat 8 & 9 Collection-2 Level-2 products. The raw data values associated with the acquired products did not align with values expected for properly atmospherically corrected surface reflectance products. To address this, we acquired Collection-2 Level-1 satellite imagery for the Dixie fire and then used Idrisi TerrSet to atmospherically correct the data using the cos(t) method. These manually corrected images were then used to process NDVI recovery and the dNBR following the same methodology outlined above.

Atmospherically correcting the Collection-2 Level-1 products involves additional processing work, but generated more reasonable results for both NDVI trends and dNBRs. In comparison to authoritative field-validated dNBRs provided by BAER teams, the dNBRs calculated from the Collection-2 Level-1 products provided similar results, whereas dNBRs calculated from the Collection-2 Level-2 products appeared to underestimate fire severity.

Results & Discussion

Land Cover Analysis

Of the 17 study fires, six were classified as forested, seven were classified as shrubland, and four were classified as grassland (**Table 3**). Understanding the general land cover within a given region is essential in contextualizing observed NDVI values and how they change spatially over time, especially in response to disturbance such as wildfire. The severity of a disturbance is also relevant. We may expect grasslands and shrublands to be more vulnerable to low-intensity fires, but have the capacity to recover relatively quickly. In comparison, a forested area may look virtually unchanged when viewing imagery following a low-severity fire, where the fire does not impact the canopy. However, in the case of a high-severity wildfire in a forested region, we expect the burned area to take decades to recover. While ecological recovery for forested ecosystems is expected to be a slow process, this is complicated by the tendency of invasive species, especially annual grasses, to "invade" burned areas, shifting the ecological assemblage and subsequently, the fire regime within the burned area (Fusco et al., 2019).

Table 3. Results for each study fire explored in this study, including the study fire year/name, acres burned, dominant landcover type, the number of annual NDVI images acquired within the growing season, and the number of years required for post-fire NDVI to return to pre-fire NDVI conditions. Fires are sorted by cover type and then by acres in descending order.

STUDY FIRE	ACRES	COVER TYPE	NDVI SAMPLES	NDVI RECOVERY (years)
2021 Dixie (CA)	963,405	Forest	4	5
1988 North Fork (WY)	565,116	Forest	36	10
1988 Canyon Creek (MT)	167,875	Forest	36	5
2015 River Complex (CA)	77,414	Forest	10	10
1996 Lone (AZ)	60,574	Forest	28	10
1993 Brush (NM)	39,349	Forest	31	5
2015 Soda (ID)	283,626	Shrub	10	0
1992 Foothills (ID)	228,076	Shrub	32	3
1996 Leamington Complex (UT)	158,029	Shrub	28	10
1999 New Pass Complex (NV)	172,226	Shrub	25	10
1996 Simnasho (OR)	117,964	Shrub	28	20
2015 Whitetail (AZ)	33,626	Shrub	10	2
1993 Wapati Peak (CO)	20,857	Shrub	31	20
2015 Butte (CA)	70,854	Grass	10	15
2015 Bear Creek (MT)	67,292	Grass	10	10
2015 Cougar Creek (WA)	53,584	Grass	10	10
2016 Beaver Creek (CO)	38,395	Grass	9	10

NDVI Recovery

Investigations of annual NDVI sampled within the peak growing season reveal NDVI alone may not be suitable to assess post-fire recovery. While there was normally a strong decrease in NDVI in the year immediately after a fire followed by a slow recovery (**Figure 3**), NDVI often rebounded quickly, and occasionally even exceeded pre-fire unburned conditions within just 2-5 years (Figure 4). While this rapid rebound of NDVI may be expected for grass-dominant landscapes, it also commonly occurred in forested ecosystem types (**Figure 4**). Interestingly, grass-dominated fires often required 10-20 years to return to pre-fire NDVI conditions (**Table 3; Figure 5**). In some cases, NDVI did not decrease in the year after a fire and in the case of the Soda (**Figure 6**) and Foothills fires, NDVI appeared to have little response to the fire disturbance and was even slightly elevated during the year of the fire.

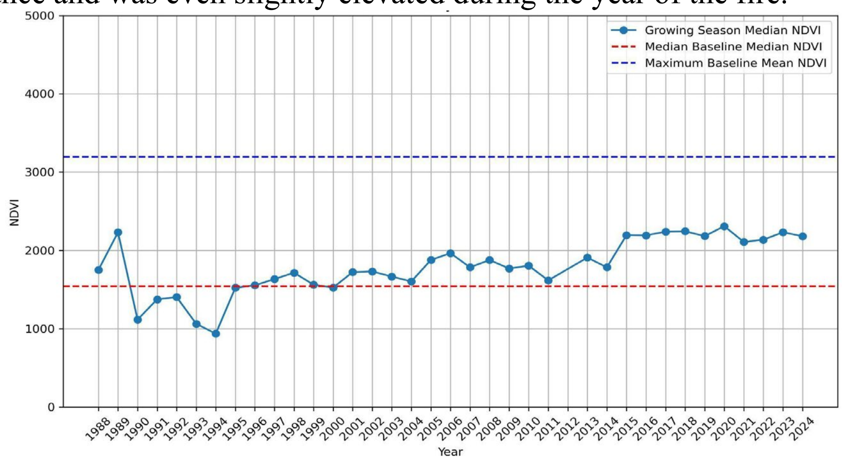

Figure 3. Annual average NDVI trend calculated within the 1988 North Fork, WY fire (forest-dominated) using imagery from Landsat 8 & 9 Collection-2 Level-2. NDVI has been scaled by 10,000. Annual NDVI was acquired within the peak growing season (June and July) for the Northern Rockies GACC. The burn was first captured in the 1989 image.

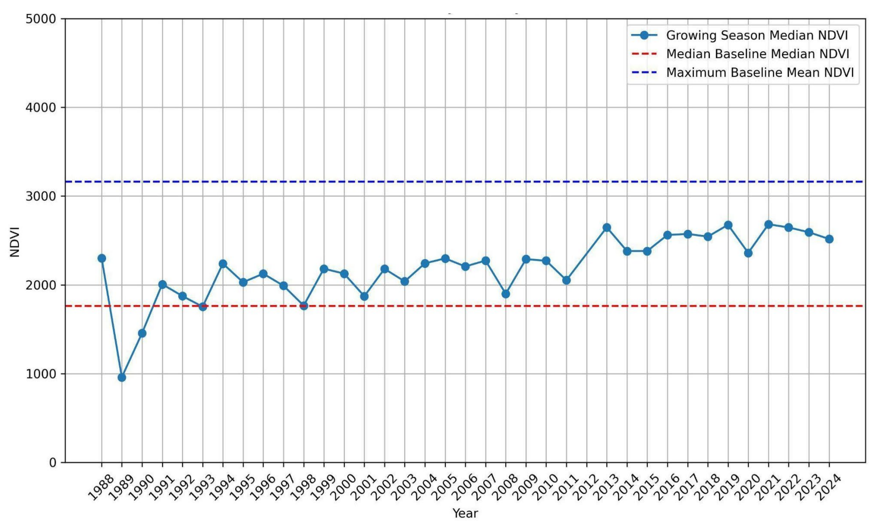

Figure 4. Annual average NDVI trend calculated within the 1988 Canyon Creek, MT fire (forest-dominated) using imagery from Landsat 8 & 9 Collection-2 Level-2. NDVI has been scaled by 10,000. Annual NDVI was acquired within the peak growing season (June and July) for the Northern Rockies GACC. The burn was first captured in the 1989 image.

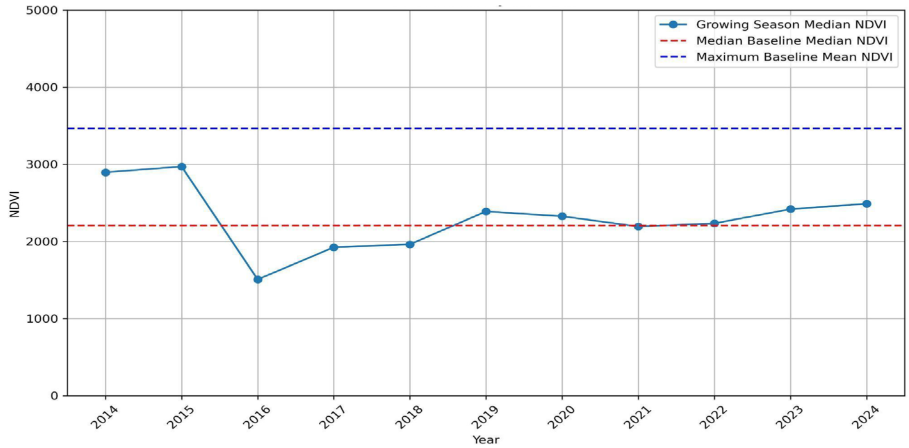

Figure 5. Annual average NDVI trend calculated within the 2015 Butte, CA fire (grass-dominated) using imagery from Landsat 8 & 9 Collection-2 Level-2. NDVI has been scaled by 10,000. Annual NDVI was acquired within the peak growing season (June and July) for the Southern California GACC. The burn was first captured in the 2016 image.

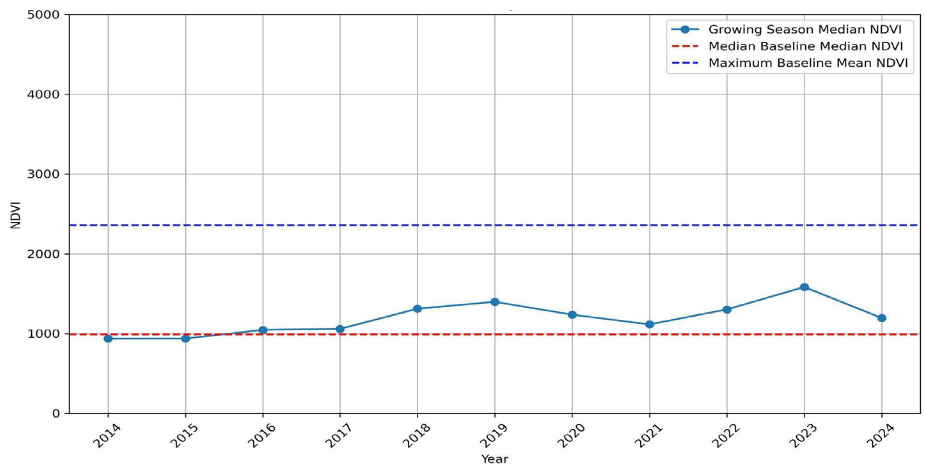

Figure 6. Annual average NDVI trend calculated within the 2015 Soda, ID fire (shrub-dominated) using imagery from Landsat 8 & 9 Collection-2 Level-2. NDVI has been scaled by 10,000. Annual NDVI was acquired within the peak growing season (June and July) for the Great Basin GACC. The burn was first captured in the 2016 image.

The mean trends in NDVI recovery time across landcover type (**Table 4**) do not realistically align with what is expected in terms of ecological post-fire recovery where forested landscapes would take longest to recover (10-20 years), shrublands would take a moderate amount of time to recover (5-10 years), and grasslands would recover fastest (<5 years). Instead, we are observing the opposite trend; forested landscapes are exhibiting the fastest NDVI recovery responses after a fire. This unexpected pattern could be due to several factors. NDVI represents the greenness of visible vegetation. In low to moderate severity burns, the forest canopy may remain intact, partially masking the burned understory vegetation and altering the perceived recovery time. Additionally, while repeat burns weren't investigated within this study, they were observed for some of the fires in the annual satellite imagery. Repeat burns may be more likely in grasslands and shrublands, which would extend the recovery time if an area burned before the NDVI recovered to pre-fire conditions.

Table 4. Mean number of years required for burned areas of each landcover type to return to pre-fire conditions based solely on NDVI response (n = 17 fires).

Landcover Type	Years
Forest	7.5
Shrub	9.3
Grass	11.3

Fire Severity

When considering the response of vegetation (as characterized by NDVI) to a fire, it is essential to also consider fire severity. Using the dNBRs for each of the study fires, we found fire severity could not completely explain the unexpected trends in NDVI recovery. For example, the large decrease and rapid recovery of NDVI following the Canyon Creek fire might be plausible if the fire had been of very low severity, primarily burning only understory vegetation. However, the dNBR describes the 1988 Canyon Creek fire as 23% moderate-low severity **(Figure 7, Table 5**), so one would expect there to be tree mortality, especially since this is a forest-dominated landscape.

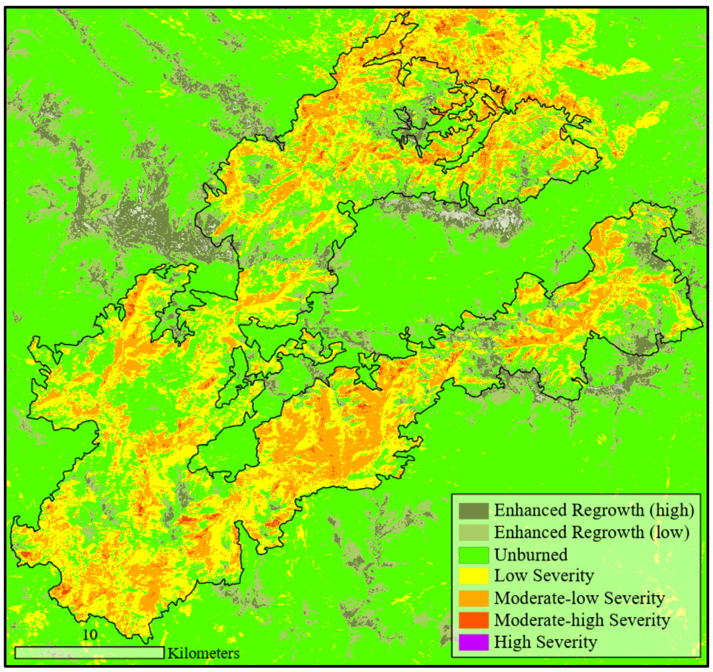

Figure 7. A dNBR calculated for the 1988 Canyon Creek, MT fire using pre-fire imagery from 7/20/1988 and post-fire imagery from 9/22/1988. Pre- and post-fire images were acquired from Landsat 4 & 5 Collection-2 Level-2.

To better understand this, NDVI response was spatially stratified by fire severity classes as defined in the dNBR for each study fire. Based on the dNBR for the Canyon Creek fire (**Figure 7**), NDVI exhibited similar trends across all severity classes, but there is an interesting association between increased fire severity and an elevated NDVI signal (Figure 8). While each severity class exhibits a relatively similar response in the year immediately following the fire, it is counterintuitive for NDVI to increase and remain elevated for moderate to high severity burn areas relative to the unburned and low severity burn areas. The simplest explanation for this relationship is that lower severity burned areas may have had less vegetation initially, resulting in NDVI values being consistently lower than areas with more vegetation where the fire burned more severely due to the abundance of fuel.

Table 5. Fires explored in this study, including the study fire year/name and percent burned area classification. Regrowth and unburned severity classes are not included but represent the remaining percent of the burned area for each fire. Percent in each severity class was determined from the dNBR in which the pixels within each severity class were compared to the total number of pixels within the fire perimeter.

STUDY FIRE	Low Severity	Mod-Low Severity	Mod-High Severity	High Severity
2021 Dixie (CA)	29%	24%	17%	2%
1988 North Fork (WY)	49%	13%	< 1%	< 1%
1988 Canyon Creek (MT)	36%	23%	1%	0%
1993 Brush (NM)	11%	1%	0%	0%
1996 Lone (AZ)	46%	31%	1%	0%
2015 River Complex (CA)	8%	1%	< 1%	0%
1992 Foothills (ID)	53%	4%	< 1%	0%
1993 Wapati Peak (CO)	3%	< 1%	0%	0%
1996 Leamington Complex (UT)	68%	3%	0%	0%
1996 Simnasho (OR)	64%	4%	< 1%	0%
1999 New Pass Complex (NV)	67%	1%	0%	0%
2015 Soda (ID)	52%	8%	< 1%	0%
2015 Whitetail (AZ)	< 1%	0%	0%	0%
2015 Butte (CA)	59%	22%	< 1%	< 1%
2015 Bear Creek (MT)	20%	< 1%	0%	0%
2015 Cougar Creek (WA)	27%	2%	0%	0%
2016 Beaver Creek (CO)	44%	35%	3%	0%

A similar relationship was observed across all 17 study fires, though in the case of the 1992 Foothills fire, NDVI within moderate and low-severity burn areas experienced short-term increases in NDVI while higher severity classes decreased, possibly indicating a repeat burn during 2004. However, the absolute NDVI values still remained high within the high severity classes relative to the lower burn severity classes (**Figure 9**).

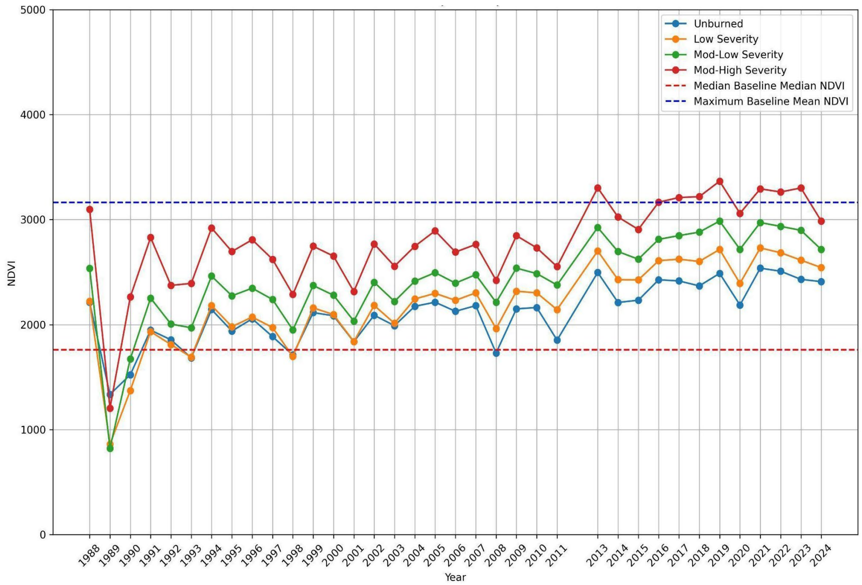

Figure 8. Annual average NDVI within each fire severity class for the 1988 Canyon Creek, MT fire NDVI values have been scaled by 10,000 with imagery acquired during the peak growing season (June and July) for the Northern Rockies GACC. The burn was first captured in 1989 imagery.

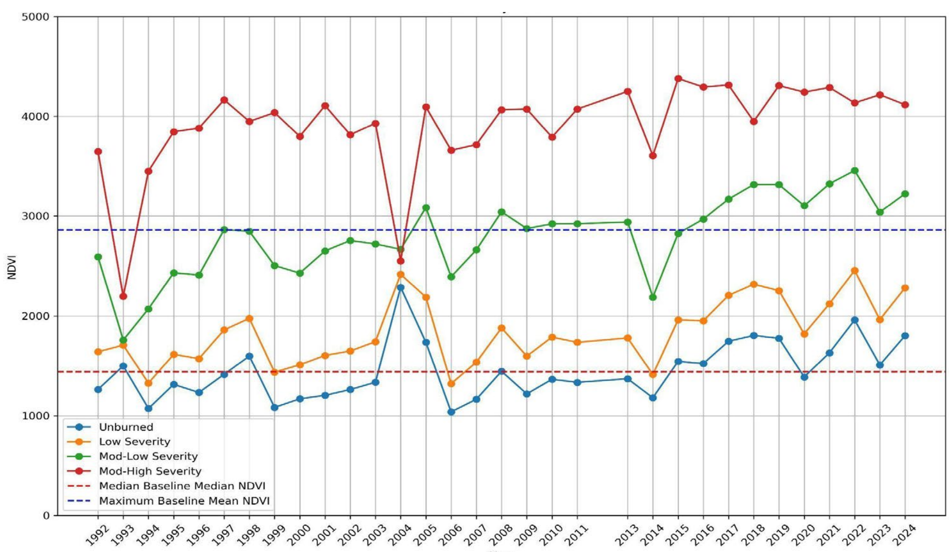

Figure 9. Annual average NDVI within each fire severity class for the 1992 Foothills Fire, ID. NDVI has been scaled by 10,000 with imagery acquired within the peak growing season (June and July). The burn was first captured in the 1989 image.

Case Study: 2021 Dixie Fire

Using the Existing Vegetation Type (EVT) dataset (LANDFIRE, 2023), we determined the burned area for the 2021 Dixie fire was forest-dominated with some shrubland. It is worth noting that the general tree species found in this region (e.g., white fir *(Abies concolor)* and red fir *(Abies magnifica)*) (**Figure 10**) are not particularly fire-resistant.

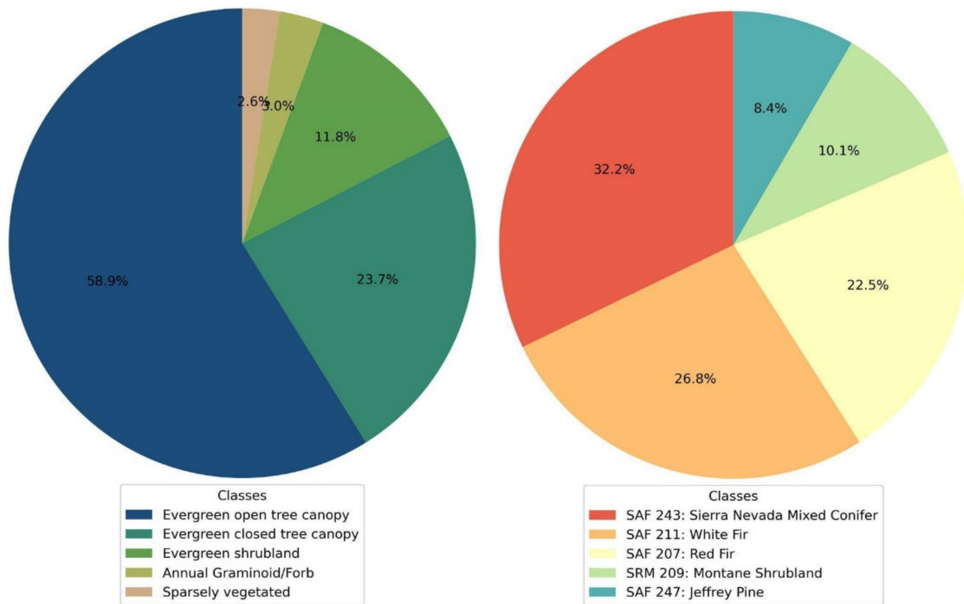

Figure 10. Top five Existing Vegetation Types (left) and Society of American Foresters/Society for Range Management cover classes (right) within the burned area of the 2021 Dixie fire in California. The burned area primarily consists of forested lands, with some shrub cover.

Overall, the 2021 Dixie fire was a relatively high-severity fire in comparison to the other study fires (Table 5). The fire has been reported as ⅓ high severity and ⅔ low to moderate severity (NPS), which doesn't align with the dNBR calculated using pre- and post-fire imagery acquired from Landsat 8 & 9 Collection-2 Level-1 imagery (**Figure 11**). This discrepancy is expected, as it is standard for official dNBR products to be corrected using field observations of the burned areas to assess fire severity. These field observations are essential to generating proper fire severity maps, but initial non-corrected dNBRs can still be useful to estimate fire severity in the absence of field verification. Field-monitoring efforts by USDA Forest Service are ongoing for the Dixie fire. This study focused on remote sensing applications and field monitoring results are not reported here.

The initial NDVI analysis for the 2021 Dixie fire describes a relatively small to moderate decrease in NDVI in response to the burn, followed by a relatively quick recovery, in which NDVI recovered by nearly 50% in just two years (**Figure 12**) and a fully recovered NDVI response within five years post-fire. This trend does not align well ecologically for a high-severity fire (**Figure 11**) in a forest-dominated landscape.

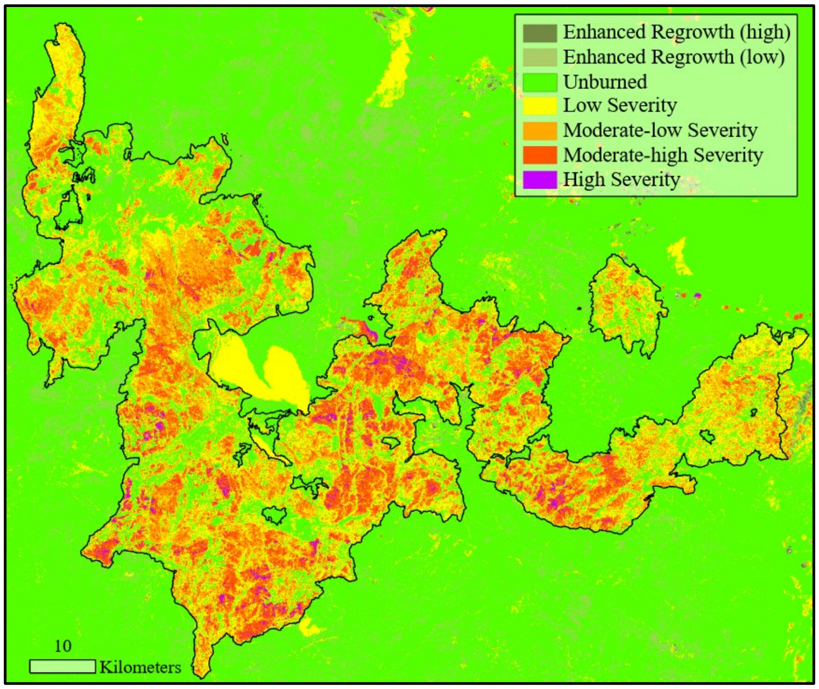

Figure 11. A dNBR calculated for the 2021 Dixie, CA fire using pre-fire imagery from 7/11/2021 and post-fire imagery from 9/29/2021. These satellite images were acquired from Landsat 8 & 9 Collection-2 Level-1, and surface reflectance was corrected for in Idrisi Terrset using the cos(T) method before calculating the dNBR.

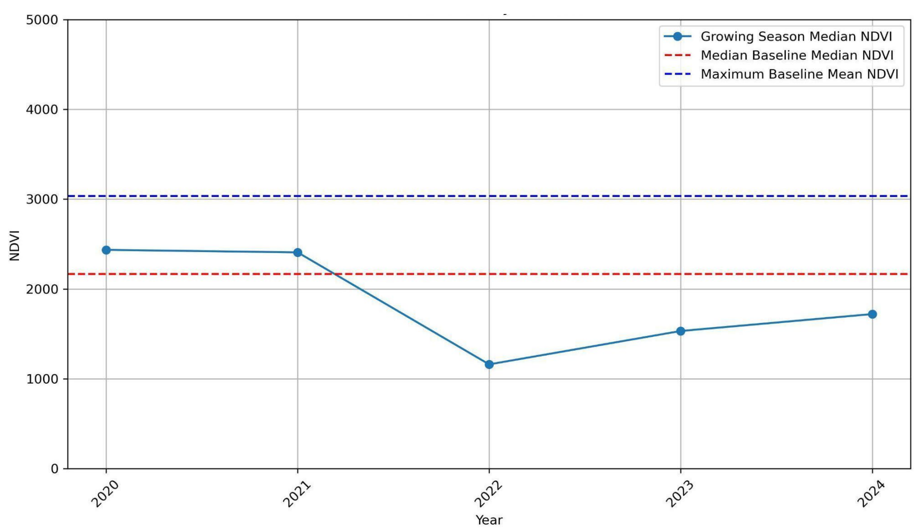

Figure 12. Annual average NDVI calculated within the 2021 Dixie, CA fire perimeter using imagery from Landsat 8 & 9 Collection-2 Level-2. NDVI has been scaled by 10,000 and imagery acquired during the peak growing season for the Dixie fire, which are the months of June and July. The burn was first captured in the 2022 image.

The second NDVI analysis for the 2021 Dixie fire used Landsat 8 & 9 Collection-2 Level-1 products which were atmospherically corrected in Idrisi TerrSet using the cos(t) method. In comparison to the previous method, the resulting NDVI trend is much better aligned with what we would expect to see for a wildfire in a forest-dominated ecosystem but it does not fit well within the NDVI Baseline dataset. This trend shows a drastic decline in NDVI in response to the fire followed by much slower recovery (**Figure 13**). If NDVI continued to recover following this trend, full vegetation recovery would be expected within 6-7 years post-fire, which is still much faster than expected for a forested ecosystem.

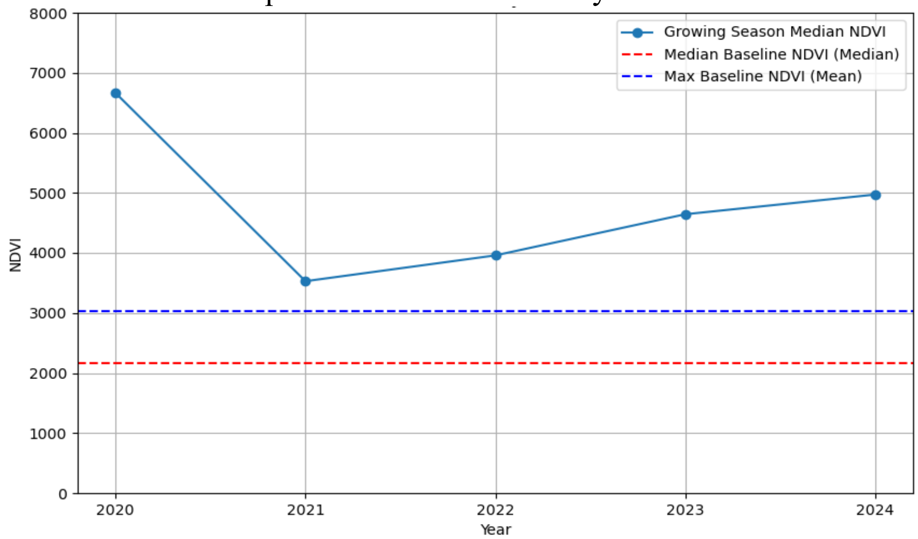

Figure 13. Annual average NDVI calculated within the 2021 Dixie, CA fire perimeter using imagery from Landsat 8 & 9 Collection-2 Level-1. Imagery was atmospherically corrected in Idrisi TerrSet using the cos(T) method before calculating NDVI and then scaled by 10,000. The y-axis on this NDVI chart extends to 8,000 whereas all other NDVI trends exist between 0 and 5,000. NDVI data were acquired within the peak growing season for the Dixie fire, (June and July). The burn was first captured in 2021 image.

LiDAR analysis reveals substantial canopy loss between 2018 and 2022 (**Figure 14**). This canopy loss is expected to represent tree removal/mortality between 2018 and 2022, which we assume is attributable to the 2021 Dixie fire. However, this assumption is based on proper spatial co-registration between the two LiDAR products (pre- and post-fire). We suspect a slight co-registration error exists between the two datasets, as there are small patches of extreme growth (e.g., 5 meters) adjacent to small patches of extreme loss (e.g., -5 meters) which are systematically consistent across the entire dataset. However, larger patterns of overall vegetation loss, no change, and vegetation growth can still be identified despite the small spatial misalignment. We suggest LiDAR data is essential for monitoring the recovery of forested ecosystems, along with NDVI, and field validation. The ability to assess canopy height changes over a broad region provides important spatial context for both the pre- and post-fire vegetation, while NDVI provides important information on the health of vegetation on the landscape. Field observations are necessary to validate and correct the results of remote sensing techniques used for burned areas.

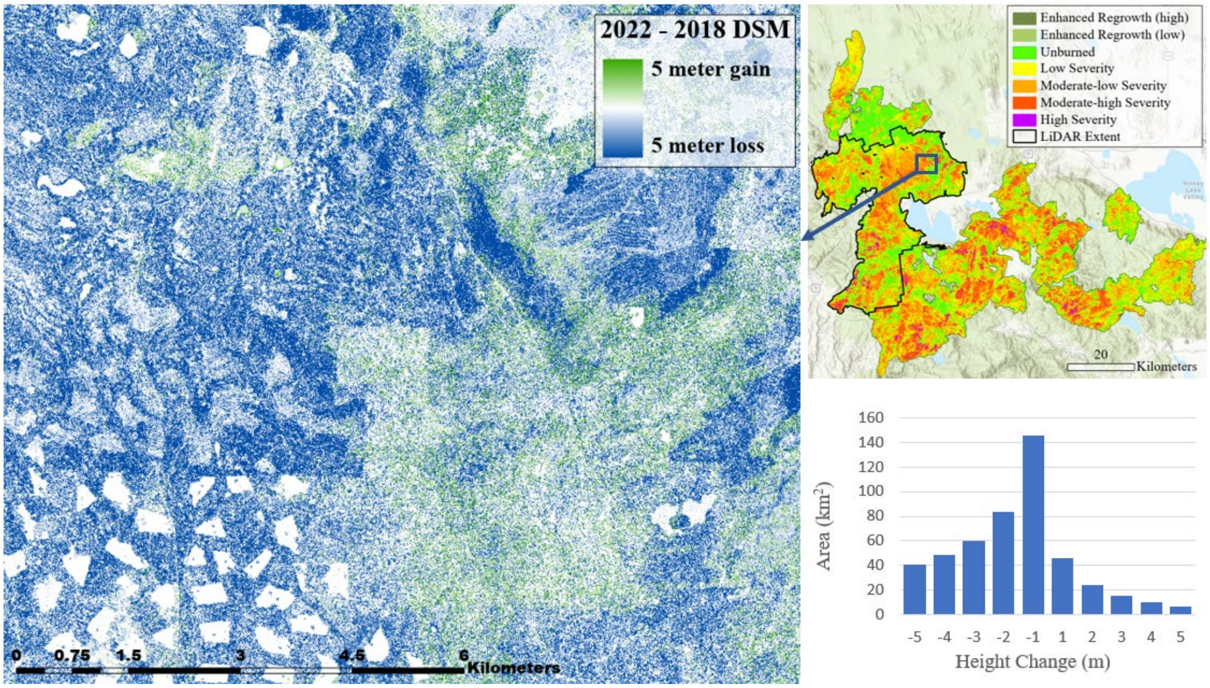

Figure 14. Map of canopy height change within a portion of the 2021 Dixie fire where both pre-fire (2018) and post-fire (2022) LiDAR data were available (indicated in the upper right extent map). Areas of no change were excluded from the histogram to illustrate gains and losses in canopy height between 2018 and 2022. The dNBR calculated for the Dixie fire is displayed within the fire perimeter in the extent map, upper right.

Conclusions

Throughout this study, we tested a methodology for utilizing NDVI to assess post-fire recovery and found that while NDVI may not be a suitable indicator of post-fire recovery on its own, it is very useful when used in conjunction with fire severity data (dNBR), LiDAR canopy height models, along with necessary field validation surveys. NDVI provides important information on the health of existing vegetation, while LiDAR is useful to understand vegetation height and structure. The combination of these remote sensing capabilities allows changes in vegetation's health and structure to be distinguished and assessed across different fire severity regions, providing a more comprehensive understanding of post-fire recovery and ecological succession.

Acknowledgements

This study was made possible through the financial support of the National Aeronautics and Space Administration (NASA) under grant award 80NSSC22K1815. The authors also thank the support of Brad Quayle and Michelle Coppoletta (USDA Forest Service) for providing data for many of the wildfires analyzed in this study.

References

Epstein, M. D., Seielstad, C. A., & Moran, C. J. (2024). Fire impact and vegetation recovery in post-fire landscapes. *Fire Ecology, 20*(1), 285, https://fireecology.springeropen.com/articles/10.1186/s42408-024-00285-9

Fusco, E. J., Finn, J. T., Balch, J. K., Nagy, R. C., & Bradley, B. A. (2019). Invasive grasses increase fire occurrence and frequency across US ecoregions. *Biological Sciences, 116* (47) 23594-23599, https://www.pnas.org/doi/full/10.1073/pnas.1908253116

Ju, J., Zhou, Q., Freitag, B., Roy, D. P., Zhang, H. K., Sridhar, M., … & Neigh, C. S. R. (2025). The Harmonized Landsat and Sentinel-2 version 2.0 surface reflectance dataset. *Remote Sensing of Environment, 324*(1), 114723, https://doi.org/10.1016/j.rse.2025.114723

Kowalski, K. J. & Weber, K. T. (2024). Comparing NDVI Across Geographic Area Coordination Centers. Idaho State University GIS Training and Research Center, https://giscenter.isu.edu/pdf/PDF_NASA_RECOVER2/NDVI_AnalysisByGACC.pdf

Lacouture, D. L., Broadbent, E. N., & Crandall, R. M. (2020). Detecting Vegetation Recovery after Fire in a Fire-Frequented Habitat Using Normalized Difference Vegetation Index (NDVI). *Forests, 11*(7), 749, https://doi.org/10.3390/f11070749

LANDFIRE. (2023). Existing Vegetation Type Dataset, LF 2.4.0, https://landfire.gov/vegetation/evt

NASA Earth Observatory. (2000). Measuring Vegetation (NDVI & EVI), https://earthobservatory.nasa.gov/features/MeasuringVegetation/measuring_vegetation_2.php

NASA RECOVER. (2023). NASA RECOVER 2.0 NDVI Baseline to Support Long-Term Post-Fire Monitoring, https://giscenter.isu.edu/pdf/PDF_NASA_RECOVER2/RECOVER_NDVI_Baseline.pdf

National Interagency Fire Center. (2024). GACC National Website Portal: About Us, https://gacc.nifc.gov/admin/about_us/about_us.htm

National Interagency Fire Center. (n.d.). Post Fire Recovery. https://www.nifc.gov/programs/post-fire-recovery

Schnase, J., Carroll, M., Gill, R., Wooten, M., Weber, K., Blair, K., May, J., & Toombs, W. (n.d.). NASA WRANGLER: Automated Cloud-based Data Assembly in the RECOVER Wildfire Decision Support System. *ISU GIS Training and Research Center*. https://giscenter.isu.edu/research/Techpg/nasa_RECOVER/pdf/schnase-igarss-1728.pdf

Stevens-Rumann, C., & Morgan, P. (2019). Tree regeneration following wildfires in the western US: A review. *Fire Ecology, 15*(1), 15, https://fireecology.springeropen.com/articles/10.1186/s42408-019-0032-1

USDA Forest Service. (n.d.). “First Returners.” https://www.fs.usda.gov/Internet/FSE_DOCUMENTS/fseprd575963.pdf

USDA Forest Service. (2006). FIREMON Landscape Assessment (LA) Sampling and Analysis Methods. Gen. Tech. Rep. RMRS-GTR-164-CD. https://www.frames.gov/documents/projects/firemon/FIREMON_LandscapeAssessment.pdf

USGS. (2018). USGS Lidar Point Cloud CA_NoCAL_3DEP_Supp_Funding_2018_D18. *USGS LiDAR Dataset:* https://rockyweb.usgs.gov/vdelivery/Datasets/Staged/Elevation/LPC/Projects/CA_NoCAL_3DEP_Supp_Funding_2018_D18/CA_NoCAL_Wildfires_PlumasNF_B1_2018/

USGS. (2022). USGS Lidar Point Cloud CA_SierraNevada_B22. *USGS LiDAR Dataset:* https://rockyweb.usgs.gov/vdelivery/Datasets/Staged/Elevation/LPC/Projects/CA_SierraNevada_B22/CA_SierraNevada_7_2022/

Weber, K. T. (2024). Historic Fires Database (HFD). *Idaho State University GIS Training and Research Center*. https://giscenter.isu.edu/research/Techpg/HFD/

Weber, K. T. (2001). A method to incorporate phenology into land cover change analysis. *Journal of Range Management, 54*(A1-A7), https://giscenter.isu.edu/research/techpg/lcc/pdf/pheno-paper.pdf
Western Fire Chiefs Association. (2023). "Ecological Succession After A Fire", Fire Ecology Wildfire Article: https://wfca.com/wildfire-articles/ecological-succession-after-a-forest-fire/. Accessed April, 2025.

Supplementary Materials

A data package containing the spatial data created for this study is available at https://giscenter-sl.isu.edu/AOC/AOC_Research/recover2/PostFireRecoveryStudy.zip